ELSEVIER

Journal of Alloys and Compounds 239 (1996) 158–171

Journal of ALLOYS AND COMPOUNDS

Synthesis of yttriumtrihydride films for ex-situ measurements

J.N. Huiberts[a], J.H. Rector[a], R.J. Wijngaarden[a], S. Jetten[a], D. de Groot[a], B. Dam[a], N.J. Koeman[a], R. Griessen[a], B. Hjörvarsson[b], S. Olafsson[b], Y.S. Cho[c]

[a]*Faculty of Physics and Astronomy, Free University, De Boelelaan 1081, 1081 HV Amsterdam, Netherlands*
[b]*Department of Physics, University of Uppsala, Uppsala, Sweden*
[c]*Department of Science Education, Kangwon National University Chuncheon, Kangwon, South Korea*

Received 23 February 1996

Abstract

A new method has been developed to synthesize compact yttriumtrihydride by making use of a thin film technique. For electrical measurements yttrium films of typically 500 nm thickness are covered under UHV conditions by a 5 nm thick palladium overlayer which consists of electrically disconnected islands. Loading of these films with hydrogen up to the trihydride phase can then be done ex-situ in a reasonably short time (around 20–40 h) by applying gas pressures of about 60×10^5 Pa. For a thicker Pd layer (above 20 nm) this time can be considerably shorter ($t \sim 125$ s). The film morphology stays intact during the loading process although the film thickness increases by approximately 11% and the crystal structure changes from h.c.p. to f.c.c. and back to h.c.p. These samples are, therefore, very well suited for an investigation of the remarkable electrical and optical properties of trihydrides, as recently reported by Huiberts et al. (*Nature, 380,* 1996, 231). In this article we give evidence for the island structure of the palladium overlayer and make a comparison of a number of physical properties of yttrium and its related hydrides as thin films with literature values for the same material in bulk form. These properties include lattice parameters for the different hydride phases, electrical resistivity for yttrium and its dihydride and Hall coefficient for yttrium. The characteristics of the yttriumhydride thin films are very similar to those of bulk material. Furthermore, we performed concentration measurements and resistivity measurements during hydrogen loading. It is shown that the resistivity rises three orders of magnitude when yttrium is loaded up to the trihydride phase at 60×10^5 Pa.

Keywords: Hydrogen in metals; Metallic films; Characterization; Trihydrides; Metal–insulator transitions

1. Introduction

Trihydrides are among the most remarkable metal–hydrogen systems. Because of the large amount of absorbed hydrogen, there are drastic changes in their electrical and structural properties. So far, only properties such as the specific heat [1], magnetic order [2], electronic [3,4] and crystal structures [5] could be investigated quite extensively [6]. Measurements of the electrical properties, however, were always complicated by the rapid oxidation rate of the parent metals and by the fact that the trihydrides could only be produced in the form of powders. Direct measurements were performed on single crystals but only up to the composition $MH_{2.75}$ [7]. Q factor resistivity measurements [8] were carried out for LaH_{2+z} with higher concentrations ($0.80 < z < 0.90$) [19], but the absolute resistivity values were only accurate within a factor of 2 or 3.

In this paper we present a simple alternative method to synthesize trihydride samples which are suitable for direct measurements of the resistivity, Hall coefficient, optical transmission/reflection or any other physical quantity requiring compact samples. A detailed description of the preparation and characterization of these samples is presented. We also show that the electrical properties of our YH_x films are essentially the same as those of bulk samples with the same composition. This comparison is of course only possible as far as bulk data are available. The good agreement confirms the quality of our samples which can, therefore, be used with confidence for a detailed study of electrical, galvanomagnetic and optical properties. Very recently we reported on optical and electri-

0925-8388/96/$15.00 © 1996 Elsevier Science S.A. All rights reserved
PII S0925-8388(96)02286-4

cal properties for YH_x with x up to 3 [10], while in the future we will report on electrical measurements for YH_x with x up to 3, in fields up to 7 T and temperatures from 4 to 360 K at hydrogen pressures up to 10^8 Pa. In particular we were able to demonstrate that YH_3 is a large gap semiconductor and that near the metal–insulator transition the optical properties change so drastically that it can be used as a switchable mirror (YH_2 is metallic and shiny while $YH_{3-\delta}$ is semiconducting and transparent).

The central idea of our method is to use a thin Pd overlayer to enhance hydrogen absorption as first proposed by Pick et al. [11] for Group V transition metals. They found that at 500 K the sticking coefficient of H on Ta increased to unity when it was covered by a palladium overlayer of more than five monolayers. They also noticed that the Pd overlayer greatly enhanced the hydrogen sticking coefficient for Nb at lower temperatures (310 K). That hydrogen loading in yttrium up to the stoichiometric trihydride can be performed at room temperature was first predicted by Yannopoulos et al. [12].

The use of the overlayer enables us to perform ex-situ measurements in contrast with early measurements on trihydride forming thin films (e.g. Y [13–15], Ho [16], Er [17], Tb [18]) which had to be loaded in an ultra-high vacuum system. In the past the loading was done by exposing the films to a hydrogen atmosphere at either room temperature [13–15] or elevated temperatures [16–18] (around 570 K) after evaporation of the base metal. At room temperature the loading times (to reach the trihydride) were extremely long (days) while in the second loading type (at high temperatures) the films turned into powder before reaching the trihydride phase. Furthermore, the hydrogen uptake slowed down considerably above the dihydride phase, possibly due to oxidation of the surface. As we were originally interested in synthesizing truly stoichiometric trihydride YH_3 for investigations under high hydrogen pressure (in the 10 GPa range in a diamond anvil cell), such an in-situ method is not well suited. For this purpose it is essential that the films can be removed from the UHV system after deposition and transferred to our cryogenic hydrogen high pressure system.

This paper is organized as follows. In Section 2 we describe the yttrium film deposition and the use of the palladium caplayer (2.1). Furthermore we describe the experimental techniques used in this work to load the samples with hydrogen (2.2), determine the hydrogen concentration (2.3), measure the resistivity and the Hall coefficient (2.4). Section 3 reports the experimental results. It starts with an optimization of the palladium caplayer (3.1) and some results concerning oxidation (3.2). This is followed by the hydrogen concentration (3.3), X-ray (3.4) and resistivity measurements during (3.5) and before (3.6) hydrogen loading. A short subsection is dedicated to resistivity measurements near the dihydride phase (3.7), the increased residual resistivity of our films (3.8) and Hall measurements (3.9). Conclusions are given in Section (4).

2. Experimental

2.1. Film preparation

Yttrium films were evaporated on Al_2O_3 substrates under UHV conditions by means of an electron gun. The purity of the yttrium base material was 99.9% and the main impurities 0.061% Ta and 0.0053% Gd. The thickness of the yttrium layers was typically 570 nm. A Pd overlayer was used for : (i) the catalytic effect of Pd on hydrogen dissociation, (ii) the increase of the hydrogen sticking coefficient and (iii) the protection of the yttrium film against oxidation, which would block the absorption completely. During deposition the layer thickness was controlled by a quartz crystal microbalance (QCM). The evaporation rate was between 0.2 and 0.5 nm per second. The palladium overlayer was evaporated by thermal heating of a palladium spiral. The optimal palladium overlayer thickness was determined to be 5 nm for electrical measurements (see Section 3.1). For optical measurements we used a thicker (20 nm) Pd layer to increase the hydrogen absorption rate. The substrate was not heated during the evaporation of either the yttrium or the palladium overlayer since heating the substrate to temperatures above $T \sim 425$ K leads to an interdiffusion of the Pd overlayer into the yttrium film. The base pressure of the system during deposition was in the 10^{-7} Pa range. Apart from the pure yttrium films we also produced a number of yttrium films with 5%, 10% and 20% barium. These films are only used for the characterization of the overlayer structure. Evaporation on other substrates (diamond, suprasil, mylar, glass) showed that the choice of substrate is not a critical one. More important is the quality of the substrate surface before evaporation. Proper cleaning (aceton, HNO_3) is necessary to avoid blistering of the film. Especially the presence of water on the surface must be avoided. Before evaporation we performed a prebake of the substrate in UHV for about 10 h at $T \sim 500$ K.

2.2. Hydrogen loading

For the present investigation the loading of the films with hydrogen was done by applying hydrogen gas pressures p_{H_2} up to a maximum of 60×10^5 Pa at room temperature. For measurements of e.g. electrical resis-

tivity and Hall effect as a function of temperature, the gas pressure was kept constant as no information about the pressure–composition isotherms of the system were available for temperatures below 500 K. It was thus impossible to adjust the pressure during the temperature sweep so as to keep the hydrogen concentration in the sample strictly constant. As the hydrogen absorption process in yttrium is exothermic the concentration should increase with decreasing temperature. However, for a material such as $YH_{3-\delta}$ the hydrogen concentration remains nearly constant since the hydrogen diffusion timescale at the temperatures of interest ($T < 350$ K) is longer than the timescale of the temperature sweep. Furthermore, at high hydrogen concentrations it follows from the high temperature solubility isotherms that there is hardly any change in composition with pressure. This was substantiated by resistivity measurements in which a YH_x film was cooled down (1 K min) at $p_{H_2} = 60 \times 10^5$ Pa hydrogen gas pressure and subsequently heated up in 1×10^5 Pa pure helium gas after evacuating the hydrogen gas. Comparing resistivity measurements performed in this way with those when the same sample was both cooled down and heated up at 60×10^5 Pa hydrogen gas pressure showed, even in this extreme case, no significant differences below 300 K. As the resistivity is directly related to the hydrogen concentration we conclude that the effect of hydrogen diffusion and concentration changes during a temperature sweep are very small for $p_{H_2} > 1 \times 10^5$ Pa.

To apply pressures up to 60×10^5 Pa at temperatures down to 2.0 K we constructed a cryogenic pressure cell. The sample holder made of copper is about 10 cm long and has a diameter of 8.0 mm. It can accommodate one sample and two thermometers. Temperatures were measured by using a Pt100 resistance thermometer for high temperatures and a 100 kΩ RuO_2 thick film resistance thermometer for low temperatures ($T < 40$ K). One of the problems with the use of Pt100 thermometers in a hydrogen atmosphere is that platinum adsorbs hydrogen at the surface, which results in a resistance increase. This problem is, however, relatively easy to cope with because the temperature derivative of the resistivity does not change. The Pt100 thermometer behaves as if hydrogen had peeled off a thin layer from the resistor wire.

2.3. Hydrogen concentration measurements

Hydrogen concentration measurements were performed with a QCM [19]. This method proved to be reliable even in situations with small absorbing volumes, e.g. in absorption and adsorption studies on palladium [20]. By applying a high frequency electric field a quartz crystal can be brought into a fundamental resonant mode at typically 6 MHz. This frequency (f_{res}) depends on the mass which is mechanically connected to the crystal. It is thus possible to measure small mass changes by monitoring the shift of the resonance frequency. In this way we determined the amount of yttrium atoms during evaporation as well as the amount of hydrogen absorbed in the yttrium film during loading. The maximum frequency shift caused by hydrogen absorption is approximately 6×10^2 Hz. For hydrogen concentration measurements a 532 nm thick yttrium film was evaporated on the electrode of a quartz crystal and subsequently covered with a 52 nm thick palladium overlayer. After the evaporation we mounted the crystal on an especially designed holder attached to a high pressure system. Hydrogen absorption measurements were performed at room temperature up to $p_{H_2} = 40 \times 10^5$ Pa. Corrections had to be made on the observed resonance frequency shift because of the change in coupling of the crystal with the surroundings due to the increasing hydrogen gas pressures [21]. This was empirically established by measuring resonance frequency changes of a quartz crystal without a yttrium film, both as a function of hydrogen and helium gas pressure. Before hydrogen loading we measured again the frequency shift for the quartz crystal with the yttrium film under helium pressure (p_{He}). The fact that the crystal was covered with a yttrium film had no effect on df_{res}/dp_{He}, so that we can use the corrections due to hydrogen gas pressure as measured for the uncovered crystal. These corrections are of the order of 2×10^2 Hz. As expected this value turns out to be approximately the same for different crystals. The starting hydrogen concentration in yttrium was established (i) by analyzing the resistivity data before loading and (ii) by X-ray measurements of a similar film after evaporation under the same conditions. The hydrogen concentration in palladium was established from previously performed measurements on Pd thin films [22]. The palladium overlayer should not have any influence on the pressure–composition isotherms of yttrium at equilibrium since the chemical potential of H in Pd is equal to the chemical potential of H in yttrium. The total relative uncertainty arising from noise in the frequency measurement and the error in the thickness determination amounts to 1.5%.

A completely different source of uncertainty in the hydrogen concentration is related to the structural phase changes (Y is h.c.p., YH_2 is f.c.c. and YH_3 is again h.c.p.). During such a phase transition the elastic properties of the material change and induce (at constant mass) a frequency shift. The error caused by this effect is small. According to Maier-Komor [19] the error is smaller than 1% up to a coverage of 4.0 mg cm^{-2}. However, one should realize that this error applies to the *total* mass of the sample, and since

the change in mass due to hydrogen uptake is only a small portion of the total mass the error in the determination of the amount of hydrogen can in principle be considerable. The coverage in our case is 0.25 mg cm^{-2} and from theory the error in the total mass is then smaller than 0.1%. This means that in principle one might expect shifts of the measured concentration as high as 0.09 near the trihydride phase. This "worst case analysis" applies to a case where the elastic properties vary in a very strong way during the phase transition. This follows from the following simple equation [19] for the mass change Δm:

$$\Delta m = \frac{1}{2} Z_Q \left(\frac{1}{f_f} - \frac{1}{f_i} \right) \quad (1)$$

where Z_Q is the elastic constant of quartz, and f_i and f_f are the frequencies respectively before and after the mass change. The elastic constant is given by the equation $Z = \rho v$ where ρ is the density and v the velocity of sound. In the case of a "reasonable" value for YH_3 ($Z_{YH_3}/Z_Q \sim 1.5$), the mistake made by using Eq. (1) is negligible. If, however, the trihydride has a more exotic value for the elastic constant ($Z_{YH_3}/Z_Q \sim$ 3.5 can be used as an upper boundary) we get the above-mentioned shift of 0.09 which represents a 3% error in $x = $ Y/H near the trihydride composition.

To protect totally the yttrium film (with a diameter of 4.5 mm) from oxidation we covered it with a palladium film of 6.0 mm diameter. Furthermore, we designed the high pressure holder in such a way that it can be attached to the UHV evaporation chamber. In this way we could measure the film thickness, as well as the oxidation after evaporation when taking the holder out of the UHV chamber, and the mass change due to hydrogen absorption during hydrogen loading. During the whole process the temperature is kept constant (and monitored as $T \sim 288$ K) by using water cooling. The oxidation process is expected to only take place at the sides of the sample were a complete coverage is difficult to attain. After taking the holder out of the UHV apparatus we wait while monitoring the oxidation until there is no detectable frequency shift. This procedure guarantees that no further oxidation takes place during hydrogen loading. At the same time we know then how many yttrium atoms have taken part in the oxidation process and are not available for the hydriding process.

To be able to check the concentrations measured by means of QCM we also determined the concentration with the ^{15}N technique [23], which makes use of a nuclear reaction between hydrogen atoms and high energy nitrogen ions. The main difference between the ^{15}N and the QCM techniques is the more local nature of the former. While in the QCM method one measures the complete mass change (due to hydrogen absorption) at any moment during absorption, the nuclear technique measures (depending on the energy of the impinging nitrogen ions) at a certain depth and gives an average over a depth interval. This interval increases (straggling effect) as we probe farther from the surface (higher energies). In our films this interval varied between 2 nm at the surface up to 20 nm at the bottom. Another important difference is that in the ^{15}N method the hydrogen concentration has to be measured in vacuum. It is then necessary to quench (down to $T \sim 180$ K) the sample to stop hydrogen absorption and desorption before measuring. In spite of these differences both measuring techniques turned out to be in excellent agreement with each other. This is an important result since the ^{15}N method is an absolute method while the QCM method requires a determination of frequency before and after hydrogen loading and is thus sensitive to the history of the loading process.

2.4. Resistivity and Hall measurements

Four-point resistivity measurements were performed in zero magnetic field between 16 and 370 K in a Thor C500 continuous flow cryostat with a temperature sweep rate of 1 K min^{-1}. The rectangular samples have a length of 11 mm and a width of 2 mm. Resistivity and Hall measurements were also carried out in an Oxford Instruments cryomagnetic system between 4 and 300 K. This Oxford Instruments system is equipped with a 7 T magnet and a hybrid bath/continuous flow cryostat. For these measurements the sample dimensions were 5 mm × 0.8 mm. For the measurement of the Hall voltage we used a vector lock-in analyzer (Princeton Applied Research model 5204) at a frequency of 62 Hz. In the metallic phase currents were of the order of 1 mA. Contacts were made by thermobonding 32 μm Al/Si wires to the yttrium films. The contact resistances between the wire and the sample were of the order of 1 Ω. In the mixed (β-YH_2)–(γ-YH_3) phase there was no influence of the current from zero to 2 mA on the measured resistivity at room temperature.

3. Results and discussion

3.1. The palladium overlayer

The palladium overlayer should satisfy two conflicting requirements: (i) it should protect the yttrium film and provide hydrogen gates to the sample and (ii) it should not affect the physical properties under investigation.

The optimal thickness of the overlayer for electrical

Table 1
Variation of the resistivity at room temperature of a 570 nm yttrium layer for three representative palladium overlayer thicknesses (19.0, 5.0 and 2.5 nm). The configuration of the samples is given schematically in Fig. 2. The resistivity is calculated for a 570 nm thickness of the yttrium layer

	Film A 19.0 nm	Film B 5.0 nm	Film C 2.5 nm
Before H_2 loading ($\mu\Omega$ cm)	151.6	157.0	238.7
After 1.0×10^5 Pa H_2 loading ($\mu\Omega$ cm)	2696.3	35179.0	239.7

measurements was determined from resistivity measurements performed on a series of samples with overlayers of various thicknesses. In Table 1 we indicate results for three representative overlayers. If the overlayer is too thick it electrically short-circuits the YH_x layer (film A). Since the effect of hydrogen on the resistivity of palladium is quite small (it only increases by a factor of 1.7 at room temperature, while the material stays metallic), the optimal overlayer thickness corresponds to the largest resistivity change upon hydrogen loading. The 19 nm overlayer is clearly too thick as there is a large influence on the resistivity in the hydrided state due to the $PdH_{0.7}$ overlayer which remains metallic while YH_3 is semiconducting. With a 5 nm thick overlayer (film B) the resistivity in the fully hydrided state at 1×10^5 Pa hydrogen pressure has increased by a factor of roughly 220. Using the measured resistivity of film A with 570 nm yttrium covered by 19 nm palladium and using the known resistivity of the palladium overlayer we can calculate the resistivity of the underlying yttrium layer.This value is equal to the measured resistivity of film B with 570 nm yttrium covered with 5 nm palladium. Hence in film B and Pd overlayer has no influence on the resistivity. If the overlayer is too thin as in film C, an impermeable Y_2O_3 surface layer forms and no hydrogen enters the underlying yttrium. From the resistivity of films C and B, and the information about the geometry of the contacts, we estimate the oxidation depth in the yttrium layer to be 200 nm.

In order to check our assumption concerning the island structure of the palladium overlayer, we synthesized a 570 nm $Y_{0.9}Ba_{0.1}$ sample and covered it with a 5 nm Pd overlayer. Barium cannot diffuse through the palladium layer and has a tendency to segregate at the surface when dissolved in yttrium in sufficient quantities. By making a depth profile of the top 10 nm of the thin film it is thus possible to obtain information about the island structure of the overlayer. Depth profile measurements performed with Auger spectroscopy show that yttrium is already present just below the surface and that a segregation of Ba takes place at the surface (Fig. 1). The measured thickness of the Pd overlayer appears to be 10 nm, which is much thicker than the 5 nm determined from a QCM measurement during evaporation of the palladium overlayer. This can only be due to the fact that the palladium is not homogeneously distributed over the yttrium film (Fig. 2). The presence of yttrium at the surface might be indicative of an alloying effect between yttrium and palladium. This will, however, not seriously disturb the hydrogen diffusion as Pd–Y alloys are highly permeable for hydrogen. Another evidence for the island structure of the 5 nm Pd layer can be found from resistivity versus temperature measurements (ρ vs. T) on the trihydride which exhibits a metal–insulator transition around 250 K, as observed in many substoichiometric trihydride systems [6,7,9] and also in superstoichiometric dihydrides (e.g. $YH_{2.10}$ [24]). A further evidence of the existence of islands is provided by atomic force microscopy (AFM) (Fig. 3). Although the palladium layer proved to be coherent just after the evaporation, owing to the high surface mobility of the palladium atoms at room temperature we get an island formation in the first hours after sample preparation (Fig. 3). Thus it can be concluded that the overlayer has no influence on the temperature dependence of ρ and that although the system must in principle be envisaged as a parallel resistor system, the palladium islands form a layer with essentially infinite resistance.

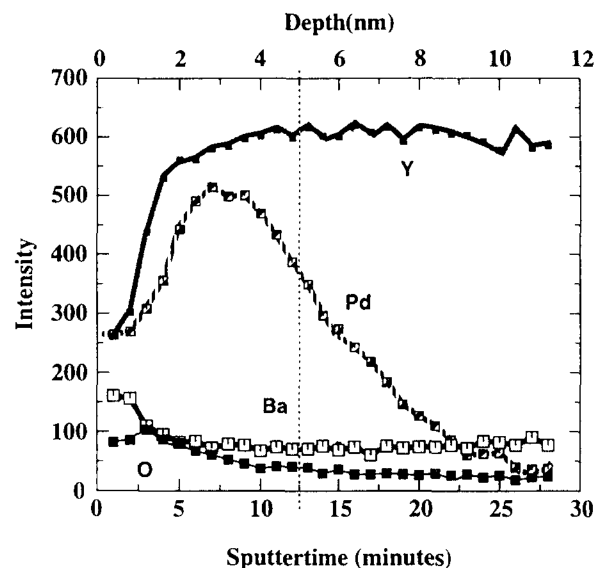

Fig. 1. Depth profile from Auger spectroscopy of a 570 nm $Y_{0.9}Ba_{0.1}$ film with a 5 nm palladium overlayer. Depth information is obtained by slowly removing the surface of the sample with 0.75 kV Ar^+-ions at a sputtering rate of 0.4 nm min^{-1} (horizontal axis). The fact that barium is able to reach the surface points to an island-like structure for the palladium overlayer. This also explains why yttrium is closer to the surface than the 5 nm expected from the thickness of the Pd overlayer.

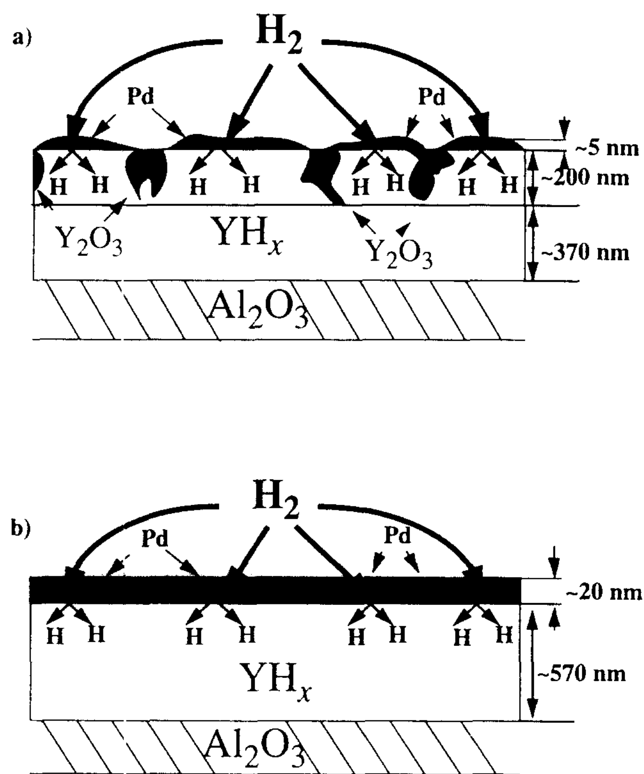

Fig. 2. Schematic cross-section of the yttrium sample with (a) the island-like overlayer structure of 5 nm thick Pd (grey), the oxidized regions are shown in black, the typical depth to which they extend is 200 nm; (b) the 20 nm thick Pd overlayer used for optical measurements, in this case yttrium is fully protected against oxidation. The substrate is Al_2O_3 (sapphire) in both cases, but a wide variety of substrates (e.g. quartz, suprasil, kapton, glass and diamond) can also be used successfully.

3.2. Oxidation

Yttrium forms one of the most stable oxides (Y_2O_3). Oxidation is therefore one of the major difficulties in the preparation of yttrium films. Since an island structure is desirable for electrical resistivity measurements (especially in the highly resistive trihydride γ-YH_3 phase) we need to investigate here the role of oxidation between the islands. In Rutherford backscattering (RBS) measurements (Fig. 4 lower curve b), oxygen is detectable up to a depth of about 175 nm. The system apparently consists of two distinguishable layers: (i) a layer of 400 nm pure yttrium and (ii) a second 175 nm thick layer which consists of a pure yttrium matrix with Y_2O_3 spikes. This is in good agreement with the oxidation depth determined from resistivity measurements on films B and C in Table 1 by assuming that the difference 238.7 − 151.6 μΩ cm is due to a reduction of the conducting cross-sectional area of the sample (i.e. 238.7 μΩ cm−151.6 μΩ cm)/238.7 μΩ cm = 0.36 ≅ (175 nm/570 nm = 0.31)). The most probable scenario is that oxygen diffuses along the grain boundaries of the polycrystalline material and subsequently obstructs further diffusion of oxygen by the formation of the Y_2O_3 phase. The influence of the Y_2O_3 spikes on the resistivity is merely to reduce the conducting thickness of the film. To correct for this effect we shall introduce below an effective thickness.

Another possible effect of the presence of oxide phase is a lowering of the maximum ratio H/Y [25]

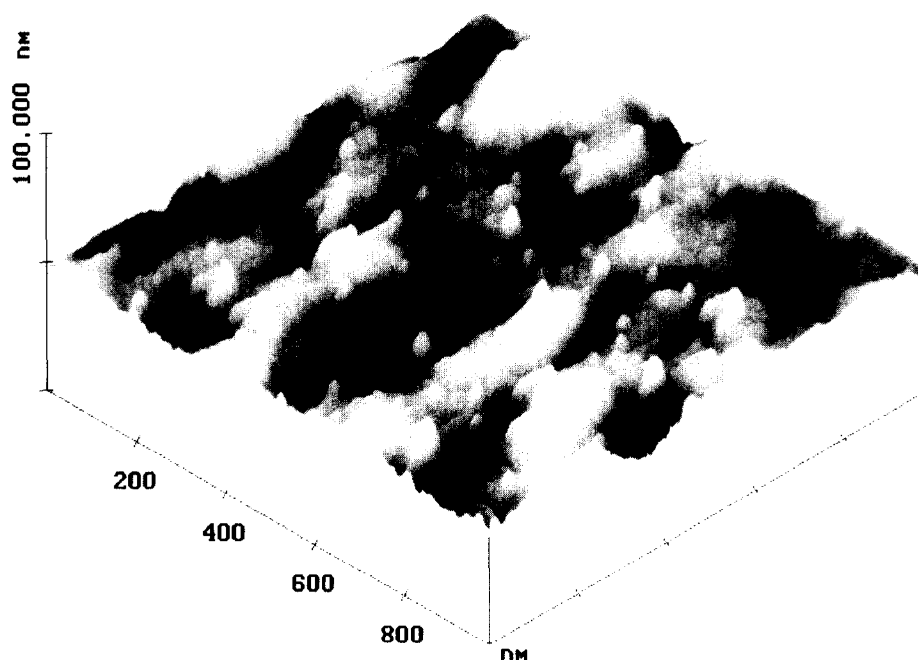

Fig. 3. 3-D AFM picture of a 500 nm Y/5 nm Pd film (length × height × width ~ 1.0 × 0.1 × 1.0 μm^3). The underlying columnar structure of the yttrium film with column diameter 200 nm is visible. The height difference due to this column growth are on the order of 20 nm. The palladium islands are visible as white "drops" on top of this structure. The drop height is between 5 and 10 nm and the width on the order of 10 nm.

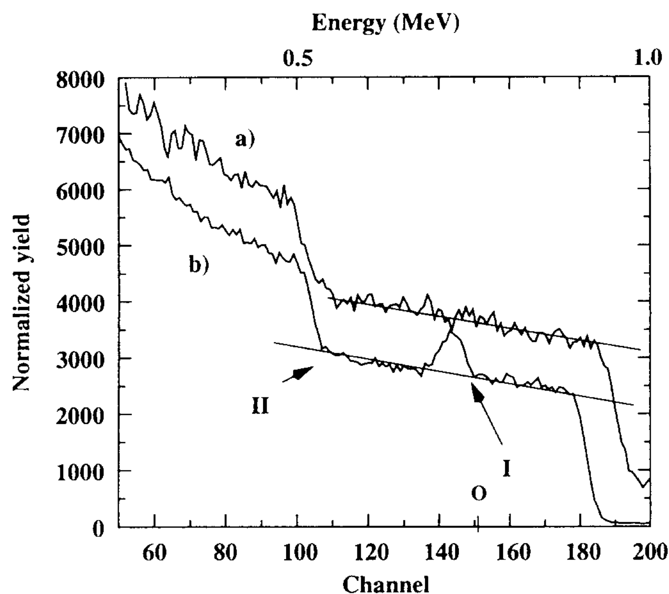

Fig. 4. Rutherford back scattering measurements on (a) a 570 nm thick yttrium film with a 5 nm palladium overlayer and (b) a 570 nm $Y_{0.8}Ba_{0.2}$ film with a 5 nm palladium overlayer. The small peak (I) in curve (b) superimposed on the background around channel 150 is due to oxygen in the sample. The fact that this peak is well separated from the oxygen signal arising from the Al_2O_3 substrate (left from point II (i.e. at energies smaller than 0.55 MeV) implies that oxygen in our sample is confined to a surface layer. In curve (a) the amount of oxygen is much lower and not visible within the resolution of the experiment.

because oxygen surrounded yttrium atoms are no longer capable of forming a yttriumhydride phase. However, RBS measurements on a sample without barium (Fig. 4 upper curve a) show that there is no detectable effect of oxygen. Similarly, ^{15}N measurements on a sample with a 5 nm caplayer and a sample with a 20 nm caplayer showed only marginal differences in the hydrogen concentration near the surface. Thus, although the oxygen has a significant influence on the effective conducting sample thickness, the total amount of oxygen in the sample remains relatively small (a few per cent in the top layer).

The residual resistivity of our thin film samples is higher than the residual resisitivity of bulk yttrium (5.95 μΩ cm at 4.2 K) [26]. Resistivity measurements on the bulk yttrium material used for the deposition of our films showed that it behaved in agreement with resistivity measurements on pure bulk yttrium as reported in the literature. The high residual resistivity of the films is, therefore, not due to impurity scattering effects apart from oxygen and possible defects in the crystal structure. As we show below it is also not due to surface scattering as the films considered here are much thicker than the mean free path of the charge carriers (see Section 3.8).

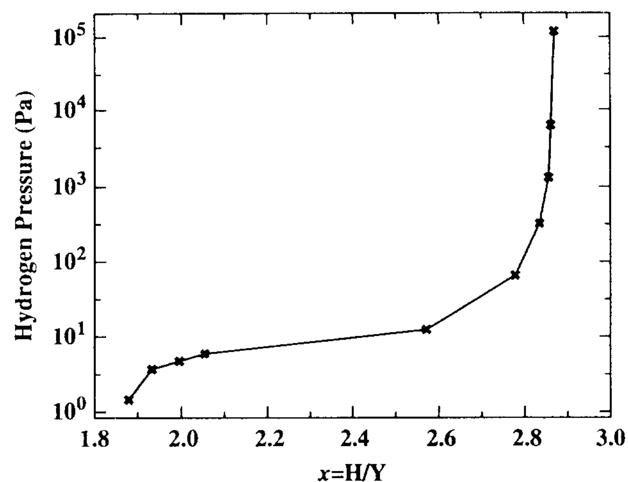

Fig. 5. Pressure–composition isotherm of a 530 nm thick yttrium film covered with a 52 nm Pd overlayer measured with a quartz crystal microbalance during hydrogen absorption at 288 K.

3.3. Hydrogen concentration

The isotherm measured by QCM measurements on a 530 nm Y/52 nm Pd at $T = 288$ K is shown in Fig. 5. Clearly visible is the (β-YH_2)–(γ-YH_3) coexisting phase plateau at a pressure of 0.092 Pa. To our knowledge this is the first isotherm ever measured for the yttrium hydrogen system at such low temperatures. The plateau pressure is relatively high compared with what is expected from an extrapolation of existing results for bulk YH_x ($2 < x < 3$). The $\Delta H_{\beta\to\gamma}$ heat of formation can be estimated from [28]

$$\frac{1}{2}\ln p_{H_2} = \frac{\Delta H_{\beta\to\gamma}}{RT} + \frac{S^0_{H_2}}{2R} \tag{2}$$

where $S^0_{H_2} = 130.81$ J K^{-1} mol^{-1} H_2 is the standard molarentropyofhydrogengasand$R = 8.314$ J mol^{-1} K^{-1} is the gas constant. With $p_{H_2} = 0.092$ Pa we obtain $\Delta H_{\beta\to\gamma} = -30.0$ kJ mol^{-1} H. Using the same procedure for bulk we obtain $\Delta H_{\beta\to\gamma} = -36.6$ kJ mol^{-1} H from the absorption isotherm at 524 K [12] with a plateau pressure equal to 0.395×10^5 Pa. The value $\Delta H_{\beta\to\gamma} = -36.6$ kJ mol^{-1} H is in reasonable agreement with more accurate values $\Delta H_{\beta\to\gamma} = -41.8$ kJ mol^{-1} H [29] and $\Delta H_{\beta\to\gamma} = -44.9$ kJ mol^{-1} H [12] determined from the temperature dependence of the plateau. The relatively high plateau pressure in Fig. 5 indicates that the heat of formation in our film is less negative than for bulk material. In other words, yttrium di- and trihydride films are slightly less stable than in bulk form.

To check effects related to a change of the elastic constant Z on QCM measurements, we also measured

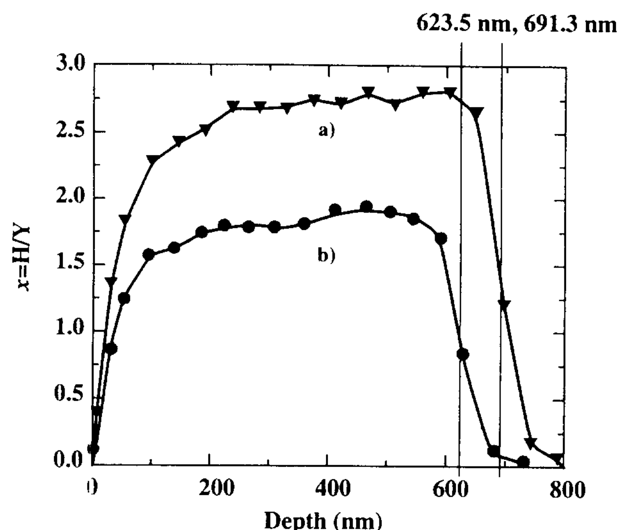

Fig. 6. Hydrogen depth profiles determined by means of the nuclear ^{15}N method for (a) a 500 nm thick yttrium film with a 5 nm palladium overlayer with $x = 2.86$ and (b) a 500 nm thick yttrium film with a 5 nm palladium overlayer with $x \sim 1.9$.

the hydrogen concentration by means of the nuclear ^{15}N method and obtained concentration profiles as shown in Fig. 6. The overall concentration H/Y for the sample determined from the measurements after loading at 1.0×10^5 Pa (top profile in Fig. 6) is 2.86 ± 0.02. The bottom curve shows a concentration profile taken at the moment where the resistivity of the sample reached its minimum value during loading. After correction for straggling the overall concentration is found to be very close to $x = 1.9$.

Both profiles in Fig. 6 indicate a somewhat lower hydrogen concentration in the top 200 nm as a result of partial oxidation near the surface. The apparent large sample thicknesses (620 and 693 nm) are due to straggling effects and strong surface roughness (around 20 nm from atomic force microscopy). Furthermore, we see a strong increase upon hydrogen loading of the sample thickness (around 11%). This value is surprisingly close to the relative volume increase (10.4%) calculated from X-ray measurements [30–33] on bulk samples when the hydrogen concentration is increased from YH_2 to YH_3. This leads to the conclusion that the entire volume expansion that occurs in bulk material is happening in the form of a one-dimensional expansion perpendicular to the film surface. This was further substantiated by AFM measurements during hydrogen loading of a typical palladium covered yttrium film. During loading the film surface moved by 50 nm (10% of the total thickness), indicating that the total volume increase is indeed taken care of by a one-dimensional expansion. Since during hydrogen absorption in bulk yttrium from Y to YH_3 the relative increase in the c-axis ($\Delta c/c = 14.6\%$) is much larger than that of the a-axis ($\Delta a/a = 0.8\%$), the one-dimensional expansion of the layer is only possible if there is a clear texture of the film.

AFM revealed also a columnar structure (diameter around 200 nm) of the film surface morphology of the yttrium film with on-top Pd islands of 10 nm diameter and between 5 and 10 nm height (Fig. 3). After hydrogen loading this top structure seems to be less sharp. An annealing process upon hydrogen absorption is possibly responsible for this surface layer smoothing.

To get a more detailed picture of the change in crystal structure upon hydrogen loading we performed X-ray measurements in the three hydrogen phases of a yttrium palladium film.

3.4. X-ray measurements

For the X-ray measurements we used a RIGAKU diffractometer with geometry similar to that for the powder method (Debye Scherrer) as our films were polycrystalline. The angle of incidence was set at 10° and the angle of reflection was varied between $\theta_0^{start} = 10°$ and $\theta_0^{end} = 65°$ ($20 < 2\theta < 75°$). X-ray measurements performed on a film in the yttrium α^*-YH_x phase (Fig. 7) indeed show that the material is randomly oriented. The calculated lattice parameters of the hexagonal yttrium phase ($a_0 = 3.657$ Å, $c_0 = 5.759$ Å) are slightly different from single phase bulk yttrium material ($a_0 = 3.650$ Å, $c_0 = 5.737$ Å) [34]. When the material is in the α^*-YH_x "solid solution" at low hydrogen concentrations the effect of hydrogen on the non-hydrogenated phase is an increase of the lattice parameters ($YH_{0.19}$: $a_0 = 3.664$ Å, $c_0 = 5.790$ Å) [30], which is in agreement with our measurements and the idea that hydrogen is incorporated during deposition. From the increase in the lattice parameters, $\Delta a_0 = 0.007$ Å and $\Delta c_0 = 0.022$ Å, we conclude that a certain amount of hydrogen is incorporated in the yttrium film during deposition [35]. From the measured Δa_0 and Δc_0 values and from the fact that $a_0 = 3.664$ Å and $c_0 = 5.790$ Å for $YH_{0.19}$ [30] we estimate that the hydrogen concentration is approximately 8.0%.

From measurements performed in the mixed (α^*-YH_x)–(β-YH_{2-z}) phase, where f.c.c. dihydride phase is predominantly present, we conclude that the measured dihydride lattice parameter ($a_0 = 5.219$ Å) is very close to the bulk value ($a_0 = 5.199$ Å [301], 5.205 Å [31], 5.201 Å [32], 5.209 Å [33]).

X-ray measurements performed on a film with β-YH_{2+z} and γ-$YH_{3-\delta}$ phases showed all the reflections from the dihydride phase. Thus the dihydride phase is randomly oriented and the influence of the substrate on the lattice parameters is small. Most reflections of the trihydride phase are also present, except that the intensity of the (100) reflection is very small. This is an

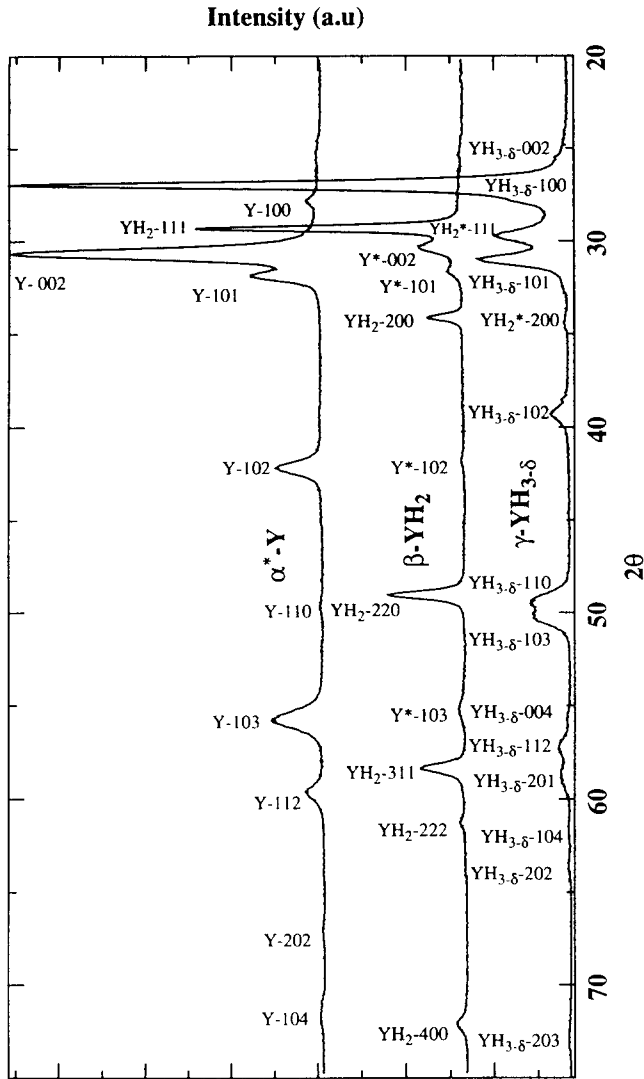

Fig. 7. X-ray spectra for a yttrium film of 570 nm thickness at different hydrogenation stages. Every peak is indexed, (hkl) notation. The asterisk indicates the presence of a second phase reflection. The maximum intensity measured is 1100 counts s^{-1} for the first peak of the YH_3 measurement. For the sake of clarity the different curves are shifted horizontally with respect to each other.

indication that the orientation of the material is not random. The texture of the trihydride phase is probably due to its hexagonal close packed structure, which is of lower symmetry than that of the face centered cubic dihydride phase. For the trihydride phase we obtained $a_0 = 3.686$ Å and $c_0 = 6.602$ Å. A comparison with bulk values $((a_0, c_0) = (3.672$ Å, 6.659 Å$)$ [31], (3.674 Å, 6.599 Å) [32], (3.672 Å, 6.625 Å) [33]) shows that a_0 is in general somewhat higher than the bulk value, while c_0 is about equal to the bulk value. One should, however, bear in mind that there may be differences in the exact hydrogen content in the samples of Refs. [30–33].

As the crystal structure of the thin films is hardly different from that of bulk material we expect that the properties of these films are representative of bulk materials, YH_2 and YH_3.

3.5. Resistivity behavior during hydrogen loading

Figs. 8 and 9 show the room temperature hydrogen loading curve of a 570 nm yttrium film covered by respectively a 5 nm and a 20 nm thick palladium overlayer at 1×10^5 Pa hydrogen pressure after having been transferred in air from the UHV deposition system into the cryostat. The 20 nm coverage is a typical value for the optical measurements. The resistivity is calculated from the measured resistance after taking into account the effective thickness d_{eff} of the sample. The effective thickness is obtained by requiring that the slope $d\rho/dT$, calculated from the resistivity versus temperature characteristic of the film before hydrogen loading, matches the slope $d\rho/dT$ [26] measured for bulk yttrium,. Although, before hydrogen loading, the anomaly at 175 K caused by a hydrogen pairing effect (after deposition we have $YH_{0.08}$ according to X-ray measurements) is clearly present, it has no influence on this procedure since $d\rho/dT$ at 50 or

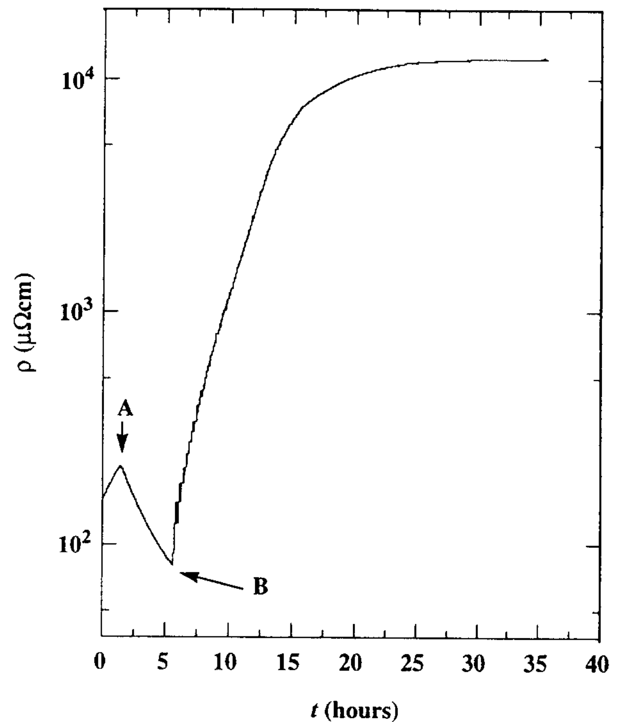

Fig. 8. Change of resistivity during hydrogen loading at room temperature and 1.0×10^5 Pa hydrogen pressure. The yttrium film is 570 nm thick and covered by a 5 nm thick palladium overlayer. At $t = 0$ s the concentration is $H/Y \approx 0.08$ since the incorporation of hydrogen is unavoidable even under UHV conditions. The rise up to point A is due to impurity scattering as the material is in the α^*-phase and the amount of hydrogen atoms rises with time. At point B the sample is (almost) pure YH_2, although there is a concentration gradient in the sample due to the slow diffusion. At $t \sim 35$ h the sample is in the γ-$YH_{3-\delta}$ phase.

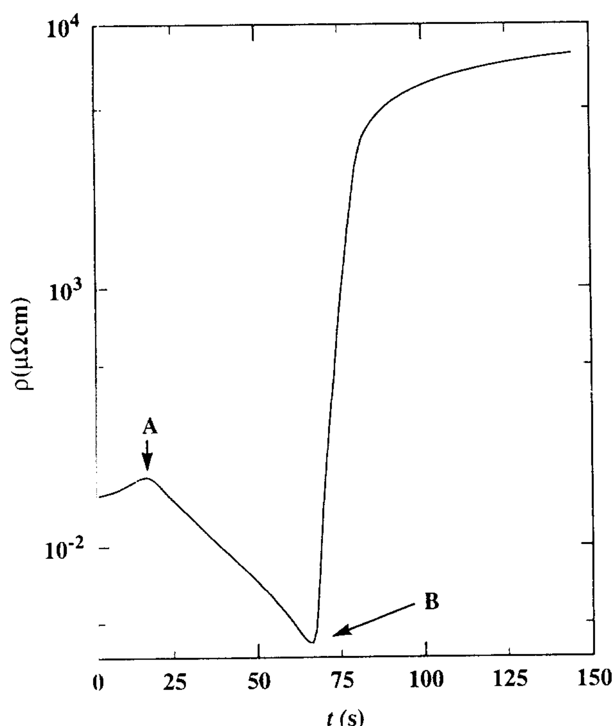

Fig. 9. Change of resistivity during hydrogen loading at room temperature and 1.0×10^5 Pa hydrogen pressure. The yttrium film is 570 nm thick and covered by a 20 nm thick palladium overlayer. At $t = 0$ s the concentration is $H/Y \approx 0.08$ since the incorporation of hydrogen is unavoidable even under UHV conditions. The rise up to point A is due to impurity scattering as the material is in the α^*-phase and the amount of hydrogen atoms rises with time. At point B the sample is (almost) pure YH_2, although there is a concentration gradient in the sample due to the slow diffusion. At $t \sim 125$ s the sample is in the γ-$YH_{3-\delta}$ phase.

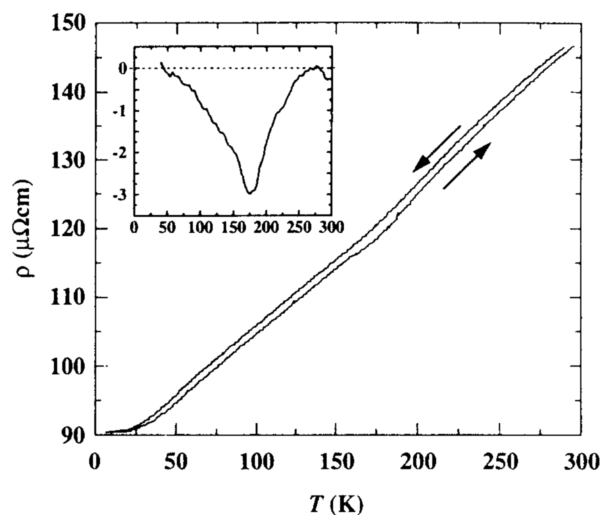

Fig. 10. Resistivity curve of a 570 nm thick yttrium film (with an effective thickness $d_{eff} \sim 465$ nm) with a 5 nm Pd cap layer before ex-situ hydrogen loading. The top curve is the resistivity during sample cooling and the lower is the resistivity during warming. The inset gives the lower curve after subtraction of a straight line which coincides with the experimental data near 50 and near 270 K. The anomaly as well as the hysteresis are due to the formation of an α^*-YH_x phase as a small amount of hydrogen, $x = H/Y = 0.08$, is unavoidably incorporated during deposition even under UHV conditions [35].

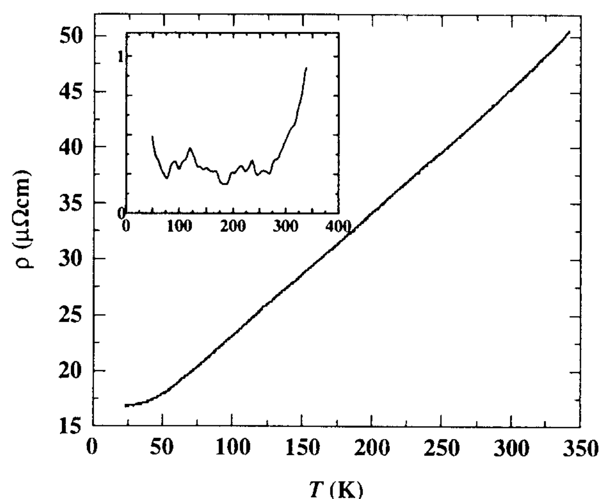

Fig. 11. Resistivity curve of the same sample as in Fig. 10 at the resistivity minimum (see point B in Fig. 8). The sample is expected to be near the dihydride phase. In the inset the same curve is depicted after a straight line subtraction. The effect of the presence of optical phonons on the resistivity is clearly visible at higher temperatures.

250 K is the same for Y and $YH_{0.08}$. The effective thickness turns out to be 465 nm. This value is used to calculate the resisitivity in the measurements in Figs. 8, 10 and 11. In Fig. 8 the resistivity increases during the first 2 h. The material is in the solid solution (α^*-YH_x) phase. The resistivity increases because of extra scattering due to the randomly distributed hydrogen atoms in the material and a decrease of charge carriers. At point A in Fig. 8 the dihydride phase precipitates and the total resistivity of the material decreases. The resistivity minimum at point B measured in this loading curve is characteristic of β-YH_2. After the minimum the resistivity rises rapidly since the trihydride is semiconducting [10]. The actual point at which the trihydride phase starts to form is, however, not easily determined from resistance measurements. As shall be discussed elsewhere, optical transmission experiments are needed to monitor the formation of the transparent semiconducting γ-YH_3 phase [10].

The relatively short loading times (20–40 h) at room temperature are due to the large absorption surface-to-volume ratio and the enhancement of absorption by the Pd overlayer. However, the absorption rate is much lower than that with a thick Pd overlayer because of the presence of the oxide phase (loading times shorter than 100 s can be reached for a 500 nm yttrium film with a 20 nm thick Pd layer). This is consistent with the diffusion coefficient $D_O \approx 6.8 \times 10^{-12}$ cm^2 s^{-1} [36] determined in dilute α^*-YH_x for octahedral–octahedral site hopping at room tempera-

ture. The time for a H-atom to travel a distance of 500 nm is then approximately $(500\,\mathrm{nm})^2/D_O \approx 368$ s.

Because of these relatively short loading times high temperatures (i.e. diffusion rates) are not necessary as they would be for bulk yttrium. Therefore thin films offer the possibility of reaching high hydrogen concentrations at modest hydrogen gas pressure, since the high x side of the β–γ coexistence region extends to higher concentrations at low temperature. An additional advantage of our thin film trihydrides is that we are able to monitor the resistivity during hydrogen loading at all times. The loading process may be interrupted at any moment to investigate the electronic properties of the material (e.g. by measuring resistivity, Hall effect, optical absorption and reflection).

3.6. Resistivity versus temperature measurements before hydrogen loading

A typical ρ vs. T curve for a 570 nm Y/5 nm Pd film before hydrogen loading is presented in Fig. 10. The anomaly at $T = 175$ K is caused by a small amount of hydrogen which is always incorporated during deposition [35]. This was also observed in the X-ray measurements mentioned before. The presence of hydrogen is unavoidable for two reasons: (i) in every ultra-high vacuum system the most abundant gas is hydrogen and (ii) yttrium is an excellent getter for hydrogen. The anomaly was previously observed in bulk material [26] with $x = \mathrm{H/Y}$ between 0.05 and 0.24 and was attributed to a pairing of hydrogen atoms below 170 K in the solid solution phase (α^*-phase). This pairing is identified as taking place along the c-axis in the hexagonal close packed structure where the neighboring sites are separated by a distance of 0.13 nm. From the deviation of the linear ρ *vs.* T behavior due to the electron–phonon interaction we can determine the Debye (θ_D) and Einstein (θ_E) temperatures and compare them with the values for bulk material [37] (Table 2). The thin film Einstein temperature is determined from the inset in Fig. 11 obtained by subtracting a straight line nearly parallel to the measured resistivity. The Debye temperature is extracted in a similar way from Figs. 10 and 11. To estimate the Einstein and Debye temperatures for the films and bulk material [37] we use the simple assumption that it is six times the temperature at which a deviation occurs in the ρ vs. T curves. The inset in Fig. 10 shows the anomaly at 175 K more clearly. From Table 2 it is clear that the Debye temperatures of Y and YH_2 are the same for our thin film as for bulk material. The Einstein temperature, which is related to the hydrogen sublattice, is higher than for bulk material. It is, in fact, comparable with values obtained by Daou and Vajda [24] for a slightly superstoichiometric dihydride with $x \sim 2.05$. It is also consistent with the neutron spectroscopy results of Udovic et al. [38], which reveal optical phonons centered around 123 meV ($\theta_E \sim 1430$ K).

Table 2
Debye and Einstein temperatures for bulk YH_x and a film of 570 nm thickness covered by a 5 nm Pd cap layer

Material	Y [37] (bulk)	$YH_{1.93}$ [37] (bulk)	Y (film)	$YH_{x\sim2}$ (film)
θ_D (K)	258 ± 2	384 ± 2	258 ± 2	372 ± 2
θ_E (K)	—	1260 ± 5	—	1698 ± 5

3.7. Resistivity versus temperature measurements near the dihydride phase

The ρ vs. T measurement for $YH_{\sim2}$ (Fig. 11) is performed at the moment when the resistivity reaches its minimum during loading (point B in Fig. 8). The anomaly at 175 K has disappeared as nearly all tetrahedral sites are filled. The Debye temperature of our thin film samples is nearly equal to the bulk material value, while the Einstein temperature is higher as can be seen in Table 2. The slope of $d\rho/dT = 0.11\ \mu\Omega\,\mathrm{cm}^{-1}\,\mathrm{K}$ is clearly larger than $d\rho/dT = 0.05\ \mu\Omega\,\mathrm{cm}\,\mathrm{K}^{-1}$ for bulk YH_2. There can be two possible reasons for this difference: (i) the observed small shift in lattice parameter of the thin film has a considerable influence on the electrical properties, and (ii) the real concentration is locally somewhat higher/lower than $x \cong 2$. The increase in slope $d\rho/dT$, increased Einstein temperature and higher residual resistivity values are in reasonable agreement with the resistivity measurements performed on $YH_{2.05}$ by Daou and Vajda [24].

3.8. Residual resistivity

As mentioned above the residual resistivity of our films is clearly higher than that of bulk YH_x, in agreement with the results of Curzon and Singh [13,14]. We show here that this is not due to surface scattering, since the thickness of the film is much larger than the mean free path. From a simple Drude model the mean free path l is given by [39]

$$l = [9.2\,\mathrm{nm}] \times [(r_s/a_0)^2/\rho_\mu] \quad (3)$$

with $r_s/a_0 = 5.44[n_{22}]^{-1/3}$ where $n_{22} = n/10^{22}$ is the charge carrier density expressed in $10^{22}\,\mathrm{cm}^{-3}$ and ρ_μ is the resistivity in $\mu\Omega$ cm. In the case of pure yttrium $n = 6 \times 10^{28}$ electrons m^{-3} at 4.2 K, as determined from the Hall measurements in Fig. 12. In the case of YH_2 we use for the charge density $1/3 \times n_Y$ to calculate the mean free path for both bulk material

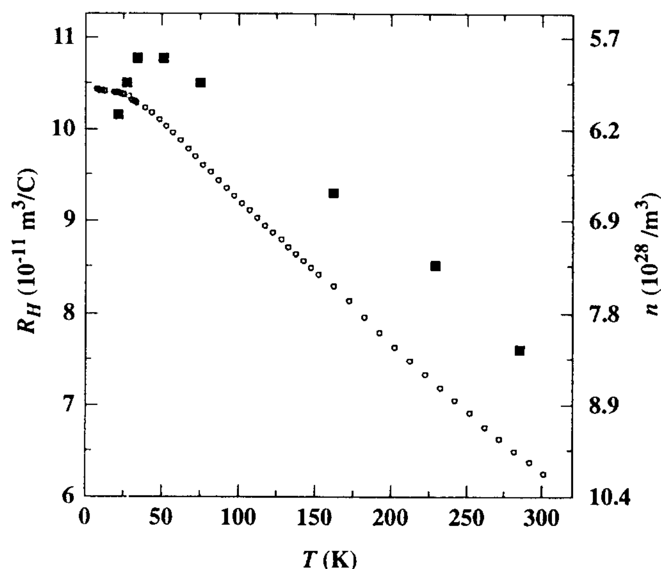

Fig. 12. Hall coefficient R_H of a 570 nm thick yttrium film covered by a 5 nm thick palladium layer. The Hall coefficient is defined as $R_H = V_H d_{eff}/BI$ with $d_{eff} \sim 500$ nm the effective thickness of the film, B the magnetic induction, I the total current through the sample and V_H the measured Hall voltage. The number of charge carriers n is calculated from the one band model expression $n = -1/R_H e$ with $e = 1.6022 \times 10^{-19}$ C. The black squares indicate the bulk values as measured by Kevane et al. [40]. The downturn in the bulk Hall coefficient data at low temperature becomes smaller and shifts towards lower temperatures after annealing of the sample.

and the films, since the Hall measurements cannot be interpreted within a single band picture due to the half occupation of the conduction band. The values of l for the film are directly calculated from the measurements shown in Figs. 10, 11 and 12. The results at $T = 4.2$ K are given in Table 3.

We consider now two effects which can be responsible for the short mean free path in film.

3.8.1. Hydrogenation during deposition

A likely candidate for raising the residual resistivity of the sample before ex-situ hydriding is the amount of hydrogen already incorporated during the deposition process itself. As we have seen from X-ray measurements (Section 3.4), approximately 8% of hydrogen is incorporated in Y during deposition. This is a direct consequence of the very large negative heat of formation YH_x ($\Delta H \sim -116$ kJ mol^{-1} H when $x \to 0$). The contribution to the residual resistivity of this 8% of hydrogen is, however, only $\rho_a = 21.5$ μΩ cm [26] at room temperature. This is far too small to explain the additional resistivity in our films, $\Delta\rho = \rho_{film} - \rho_{bulk}$ (157 μΩ cm − 57 μΩ cm ≅ 100 μΩ cm). This means that there is still a considerable effect from defect scattering and oxygen impurities. In-situ measurements on yttrium films in the UHV deposition system also showed an increased resistivity at room temperature ($\rho \sim 125$ μΩ cm [14]) for thin films thicker than 200 nm.

Table 3
Mean free path at 4.2 K in yttrium and yttriumdihydride for the bulk case and for thin films as calculated with Eq. (3)

Mean free path l (nm)	Y	YH_2
Bulk	14 [26,40]	755 [37]
Film	0.9	9.9

3.8.2. Grain boundaries

In yttrium the mean free path can be strongly influenced by grain boundaries which arise due to the columnar growth of these films (as seen by AFM). The mean free path of yttriumdihydride in the film is much larger than for yttrium. The residual resistivity of the dihydride is also clearly lower than the residual resistivity of the yttrium film after evaporation. It seems valid to conclude from these values that during the strongly exothermic hydriding process either a defect annealing of the material or a reduction of the oxide phase ($2Y_2O_3 + 7H_2 \to 3H_2O + 4YH_2$) is taking place. As the most probable location for the oxide phase is the grain boundaries, one expects that both mechanisms play a role simultaneously.

3.9. Hall measurements

For the yttrium film before hydrogenation (Fig. 12) the Hall coefficient and its dependence on temperature are in good agreement with measurements on bulk material [40]. Yttrium is an electron conductor and has a Hall coefficient $R_H = 6.2 \times 10^{-11}$ m^3 C^{-1} at room temperature and $R_H = 10.5 \times 10^{-11}$ m^3 C^{-1} near $T = 0$ K. Differences between our measurements and those of Kevane et al. [40] are probably related to the uncertainty in the effective thickness or to the disorder present in films. The anomaly at 175 K is also visible in the Hall measurement. At temperatures below the anomaly the hydrogen atoms cause a reduction of the amount of charge carriers at the Fermi level by creating s–d hybridized bands just below the Fermi level. If we set the hydrogen concentration at $H/Y \approx 0.08$, derived from X-ray measurements, the lowering of the total amount of charge carriers would be of the order of $0.08/3 \times 100\% \approx 2.7\%$, which is a small effect. The observed temperature behavior can be explained by a two band model where the ratio of the number of holes to the number of electrons can change during contraction of the lattice upon cooling [40].

Values for the Hall coefficient of the three hydrogen phases (α^*-YH_x, β-YH_2 and γ-$YH_{3-\delta}$) are given in Table 4. For the measurement in the dihydride phase the Hall coefficient is close to zero, in agreement with the fact that the band at the Fermi level is exactly half filled. We observed that this value can be either

Table 4
Measured Hall coefficient at 300 K in the α^*-YH_x, β-YH_2 and γ-$YH_{3-\delta}$ phase of the same yttriumhydride film as in Fig. 12. The concentrations marked 2_a and 2_b belong to two different measurements for the β-YH_2 phase performed around the resistivity minimum

$x = H/Y$	R_H ($m^3 C^{-1}$)
0.08	-6.2×10^{-11}
2_a	-2.5×10^{-12}
2_b	$+1.25 \times 10^{-11}$
2.873	-3.2×10^{-7}
2.887	-4.0×10^{-7}
2.898	-4.6×10^{-7}

positive (more than half occupation) or negative (less than half occupation). This behavior is quite similar to the Hall coefficient measured by Heckman [41] for CeH_2. The values for the trihydride material indicate the strong lowering in the charge density due to the opening of the semiconducting gap. It is interesting to point out, however, that the charge density in $YH_{3-\delta}$ is much smaller than what one would expect on the basis of the large concentration δ of octahedral vacancies which act as donors.

4. Conclusions

Our results show that the ex-situ synthesis of trihydrides by making use of thin yttrium films (around 570 nm) covered with a 5 nm palladium layer is reproducibly possible and enables for the first time electrical and optical measurements on a trihydride [10]. The only minor disadvantage is that in the metallic phase the residual resistivity is higher than in bulk samples due to extra disorder and a small amount of hydrogen incorporated in the thin film during deposition. The oxide phase, which is present at the surface, and the palladium overlayer do not have any effect on the temperature dependence of the resistivity. X-ray measurements show that the lattice parameters of the hydride phases are only marginally influenced by the substrate. The trihydride phase is partly oriented, while there is no orientation present in the as-evaporated yttrium film. This points to an orientational tendency during hydrogen loading.

QCM measurements are used for the determination of the first room temperature pressure–composition isotherms of YH_x. The QCM method results are in remarkably good agreement with hydrogen concentration measurements obtained by means of the nuclear ^{15}N method.

A yttrium film covered with a 20 nm Pd overlayer can be kept in air for days without a noticeable deterioration or change of properties. The film remains in the (stable) dihydride phase in which octahedral occupation plays an important role as far as optical properties are concerned. As shown elsewhere the yttrium films in combination with a palladium overlayer offer the possibility to monitor the resistivity behavior and the change in light transmission during the loading process. In this way we have a simple method to measure the electrical and optical characteristics of the hydride material in the different stages of the hydrogenation process without being confined to a UHV system.

One of the remarkable features in this work is the fact that, although there is a 13.5% expansion of the crystal lattice and two thermodynamic phase transitions occur when the hydrogen concentration is increased from essentially zero to three, the films do not deteriorate under hydrogen loading.

The thin film method described in this work is not limited to yttrium in its application. The possibility of switching rapidly, easily, and reversibly from a shiny metal (YH_2) to a transparent semiconductor ($YH_{3-\delta}$), and modifying the charge carrier density by a mere change of the ambient hydrogen pressure, might open the way to technological applications of thin layers of rare earths, yttrium and lanthanum hydrides.

Acknowledgements

We are grateful to the group of E. Karlsson (University of Uppsala) for their help with the ^{15}N hydrogen profiling measurements and to AMOLF for enabling us to perform RBS measurements. This work is part of the research program of the "Stichting voor Fundamenteel Onderzoek der Materie" (FOM), which is financially supported by NWO. One of us (Y.S.C.) is grateful to the "Non-directed Research Fund", Korean Research Foundation, 1991.

References

[1] Z. Bieganski and M. Drulis, *Phys. Status Solidi A*, *44* (1971) 91. Z. Bieganski and M. Drulis, *Phys. Status Solidi A*, *35* (1976) K127. Z. Bieganski and B. Stalinski, *Z. Phys. Chem. N.F.*, *Bd. 116* (1979) 109. K. Kai, K.A. Gschneidner, Jr., B.J. Beaudry and D.T. Peterson, *Phys. Rev. B*, *40* (1989) 6591.
[2] J.M. Friedt, G.K. Shenoy, B.D. Dunlap, D.G. Westlake and A.T. Aldred, *Phys. Rev. B*, *20* (1979) 251.
[3] A. Fujimori and L. Schlapbach, *J. Phys. C: Solid State Phys.*, *17* (1984) 341.
[4] E. Debowska, *Z. Phys. Chem. N.F.*, *Bd.*, *164* (1989) 1101.
[5] P. Klavins, R.N. Shelton, R.G. Barnes and B.J. Beaudry, *Phys. Rev. B*, *29* (1984) 5349.
[6] P. Vajda, Hydrogen in rare-earth metals including RH_{2+x} phases, in *Handbook on the Physics and Chemistry of Rare Earths*, Vol. 20, Elsevier, 1995, p. 207.
[7] G.G. Libowitz, *Ber. Bunsenges. Ges.*, *77* (1973) 837.

[8] J. Shinar, B. Dehner, B.J. Beaudry and D.T. Peterson, *Phys. Rev. B*, *37* (1988) 2066.
[9] J. Shinar, B. Dehner, R.G. Barnes and B.J. Beaudry, *Phys. Rev. Lett. 64* (1990) 563.
[10] J.N. Huiberts, R. Griessen, J.H. Rector, R.J. Wijngaarden, J.P. Dekker, D.G. de Groot and N.J. Koeman, *Nature*, *380* (1996) 231.
[11] M.A. Pick, J.W. Davenport, M. Strongin and G.J. Dienes, *Phys. Rev. Lett.*, *43* (1979) 286.
[12] L.N. Yannopoulos, R.K. Edwards and P.G. Wahlbeck, *J. Phys. Chem.*, *69* (1965) 2510.
[13] A.E. Curzon and O. Singh, *J. Phys. F: Met. Phys.*, *8* (8) (1978) 1619.
[14] A.E. Curzon and O. Singh, *Thin Solid Films*, *57* (1979) 157.
[15] P. Bracconi, E. Pörschke and R. Lässer, *Appl. Surf. Sci.*, *32* (1988) 392.
[16] M.S. Rahman Khan, *Bull. Mater. Sci.*, *9* (3) (1987) 181.
[17] M.S. Rahman Khan, *Appl. Phys. A*, *35* (1984) 263.
[18] M.S. Rahman Khan, *Ind. J. Phys.*, *55A* (1981) 23.
[19] P. Maier-Komor, *Nucl. Instrum. Meth. Phys. Res.*, *A234* (1985) 641.
[20] R.V. Bucur, V. Mecea and T.B. Flanagan, *Surf. Sci.*, *54* (1976) 477.
[21] C.D. Stockbridge, *Vacuum Microbalance Techniques*, Vol. 5, Plenum Press, New York, 1966, p. 147.
[22] G.A. Frazier and R. Glosser, *J. Less-Common Met.*, *74* (1980) 89.
[23] W.A. Lanford, H.P. Trautvetter, J.F. Ziegler and J. Keller, *Appl. Phys. Lett.*, *28* (1976) 566. W.A. Langford, *Nucl. Instrum. Meth. Phys. Res.*, *149* (1978) 1. B. Hjörvarsson, J. Rydén, T. Ericsson and E. Karlsson, *Nucl. Instrum. Meth. Phys. Res.*, *B42* (1989) 257. B. Hjörvarsson and J. Rydén, *Nucl. Instrum. Meth. Phys. Res.*, *B45* (1990) 36.
[24] J.N. Daou and P. Vajda, *Phys. Rev. B*, *45* (1992) 10907.
[25] G.M. Begun, J.F. Land and J.T. Bell, *J. Chem. Phys.*, *72* (1980) 2959.
[26] J.E. Bonnet, C. Juckum and A. Lucasson, *J. Phys. F: Met. Phys.*, *12* (1982) 699.
[27] W.M. Mueller, J.P. Blackledge and G.G. Libowitz, *Metal Hydrides*, Ac. Press, 1968, p. 443.
[28] R. Griessen and T. Riesterer, *Heat of Formation Models*, Top. Appl. Phys., Vol. 63, Springer, Berlin, 1988, Chapter 6.
[29] H.E. Flotow, D.W. Osborne, K. Otto and B.M. Abraham, *J. Chem. Phys. 38* (1963) 2620.
[30] K. Dialer and B. Frank, *Z. Naturforsch. B 15* (1960) 58.
[31] A. Pebler and W.A. Wallace, *J. Phys. Chem.*, *66* (1962) 148.
[32] C.E. Lundin and J.P. Blackledge, *J. Electrochem. Soc.*, *109* (1962) 838.
[33] H.E. Flotow, D.W. Osborne and K. Otto, *J. Chem. Phys.*, *36* (1962) 866.
[34] F.H. Spedding and B.J. Beaudry, *J. Less-Common Met.*, *25* (1971) 61.
[35] A.E. Curzon, *J. Less-Common Met.*, *98* (1984) 149.
[36] D.L. Anderson, R.G. Barnes, S.O. Nelson and D.R. Torgeson, *Phys. Lett.*, *74A*(6) (1979) 427.
[37] J.N. Daou, A. Lucasson, P.A Vajda and J.P. Burger, *J. Phys. F: Met. Phys.*, *14* (1984) 2983.
[38] T.J. Udovic, J.J. Rush and I.S. Anderson, *Phys. Rev. B*, *50* (1994) 15739.
[39] N.W. Ashcroft and N.D. Mermin, *Solid State Physics*, Holt-Saunders Japan Ltd., Tokyo, 1981, Appendix A.
[40] C.J. Kevane, S. Legvold and F.H. Spedding, *Phys. Rev.*, *91* (1953) 1372.
[41] R.C. Heckman, *J. Chem. Phys.*, *46* (1967) 2158.